HAL
archives-ouvertes.fr

Wavefront sensing for aberration modeling in fluorescence MACROscopy

Praveen Pankajakshan, Alain Dieterlen, Gilbert Engler, Zvi Kam, Laure Blanc-Féraud, Josiane Zerubia, Jean-Christophe Olivo-Marin

▶ **To cite this version:**

Praveen Pankajakshan, Alain Dieterlen, Gilbert Engler, Zvi Kam, Laure Blanc-Féraud, et al.. Wavefront sensing for aberration modeling in fluorescence MACROscopy. IEEE International Symposium on Biomedical Imaging (ISBI), IEEE Signal Processing Society, Mar 2011, Chicago, United States. inria-00563988

HAL Id: inria-00563988
https://hal.inria.fr/inria-00563988

Submitted on 7 Feb 2011

HAL is a multi-disciplinary open access archive for the deposit and dissemination of scientific research documents, whether they are published or not. The documents may come from teaching and research institutions in France or abroad, or from public or private research centers.

L'archive ouverte pluridisciplinaire **HAL**, est destinée au dépôt et à la diffusion de documents scientifiques de niveau recherche, publiés ou non, émanant des établissements d'enseignement et de recherche français ou étrangers, des laboratoires publics ou privés.

WAVEFRONT SENSING FOR ABERRATION MODELING IN FLUORESCENCE MACROSCOPY

Praveen Pankajakshan[*1], *Alain Dieterlen*[2], *Gilbert Engler*[3], *Zvi Kam*[4], *Laure Blanc-Féraud*[5], *Josiane Zerubia*[5], *Jean-Christophe Olivo-Marin*[*1]

[1] Quantitative Image Analysis Unit, Institut Pasteur, 75015 Paris, France.

[2] Laboratoire MIPS-LAB.EL, Université de Haute-Alsace, 68093 Mulhouse, France.

[3] IBSV Unit, INRA, 06903 Sophia Antipolis, France.

[4] Molecular Cell Biology, Weizmann Institute of Science, Rehovot 76100, Israel.

[5] ARIANA Project-team, INRIA/CNRS/UNS, 06902 Sophia Antipolis, France.

ABSTRACT

In this paper, we present an approach to calculate the wavefront in the back pupil plane of an objective in a fluorescent MACROscope. We use the three-dimensional image of a fluorescent bead because it contains potential pupil information in the 'far' out-of-focus planes for sensing the wavefront at the back focal plane of the objective. Wavefront sensing by phase retrieval technique is needed for several reasons. Firstly, the point-spread function of the imaging system can be calculated from the estimated pupil phase and used for image restoration. Secondly, the aberrations in the optics of the objective can be determined by studying this phase. Finally, the estimated wavefront can be used to correct the aberrated optical path without a wavefront sensor. In this paper, we estimate the wavefront of a MACROscope optical system by using Bayesian inferencing and derive the Gerchberg-Saxton algorithm as a special case.

Index Terms— fluorescence MACROscopy, phase retrieval, field aberration, Gerchberg-Saxton algorithm, Bayes' theorem

1. INTRODUCTION

The MACROscope is an imaging arrangement for analyzing microscopic and MACROscopic preparations by collecting the emitted fluorescence from a preparation [see 1]. The working principle behind such a MACROscope is similar to that of a fluorescence microscope except for (an) additional zoom lens(es). This extra attachment to the objective lens makes it possible to view large object fields and to work at larger distances. Fig. 1 shows a schematic of the MACROscope with the arrows showing the axial movement of the motorized control and the zoom lens system. By fixing the objective and changing the zoom positions, the system can work at a distance of about 80mm above the specimen and provide a 20mm (diagonal diameter) field-of-view (FOV).

In this paper, we tackle the problem of phase retrieval as it is linked to the problem of object restoration from observed intensities using a calculated point-spread function (PSF). In addition, the shape of the wavefront determines the type of aberrations during imaging and also permits its eventual correction. In literature, prior work related to this subject is on wavefront reconstruction using adaptive optics (AO) [see 2; 3; 4]. The AO methods are based on the idea of phase aberration compensation by physically adding a special conjugate element in the optical system. A review of the recent trends in AO is given in [5]. In [6], the amplitude and phase of the pupil function was measured by using a fiber-optic interferometer. We will see how wavefront sensing could also be done computationally from a Bayesian perspective and derive the Gerchberg-Saxton (GS) [7] algorithm as a special case.

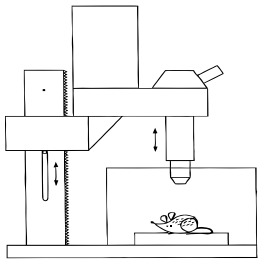

Fig. 1. Schematic of a MACROscope showing axial zoom and motorized control. Reproduced from [1].

This article is organized as follows. In Section 2, we provide the background for a scalar PSF calculation and the mathematical framework for the Bayesian interpretation. As the MACROscope's zoom is variable, for a fixed objective magnification, the working effective numerical aperture (NA) of the optical system is unknown. As a result, for the algorithm, the effective NA needs to be calculated from the images of point sources. The objective lens of a MACROscope is corrected for certain aberrations like the chromatic aberration. As the MACROscope works under very low NA (the illumination and the emission rays are nearly paraxial), the spherical aberration due to the difference in the refractive index between the objective immersion medium and the specimen medium is negligible. Nevertheless, the use of different apertures for changing the zoom can cause other aberrations. We will see towards the end of this article, in Section 3, how the retrieved phase can be used to detect such aberrations.

2. WAVEFRONT SENSING-A BAYESIAN INTERPRETATION

Wavefront sensing by phase retrieval is the process of estimating the amplitude and the phase of a pupil function from the observed intensities of a point source. In order to develop our phase retrieval

This research was supported by the ANR DIAMOND project (http://www-syscom.univ-mlv.fr/ANRDIAMOND). The authors gratefully acknowledge Dr. Philippe Herbomel (Institut Pasteur, France) and Dr. Didier Hentsch (Imaging Centre, IGBMC, France) for letting us use their MACROscopes and for the interesting discussions. We would also like to thank Dr. Mickäel Lelek (Institut Pasteur, France) for preparing the bead samples.

*Email: {praveen,jcolivo}@pasteur.fr.

algorithm, we have to look at the scalar diffraction model of the magnitude PSF. From the Kirchhoff-Fraunhofer approximation [see 8], we can write the near-focus amplitude PSF, $h_{\mathrm{A}}(x,y,z)$, in terms of the inverse Fourier transform of the two-dimensional (2-D) exit pupil function, $P(k_x,k_y,z)$, at each defocus z as

$$h_{\mathrm{A}}(x,y,z) = \mathcal{F}_{\mathrm{2D}}^{-1}\{P(k_x,k_y,z)\}\,, \tag{1}$$

where $(x,y,z) \in \Omega_s$ and $(k_x,k_y,k_z) \in \Omega_f$ are the coordinates in the spatial and in the pupil domain. The above expression states that the field distribution of a point source in an image space is the inverse Fourier transform of the overall complex field distribution of the wavefront, in the back pupil plane of the optical system. We also notice that the inverse Fourier transform of an unaberrated pupil, when considered as a circular disc, gives an Airy disc pattern (*Bessel* function). If we represent (k_x,k_y) in the radial coordinates, $\theta_i = \arcsin((k_x^2+k_y^2)^{1/2}/k_i)$ and $k_i = 2\pi n_i/\lambda_{\mathrm{ex}}$. n_i is the refractive index of the objective immersion medium and λ_{ex} the excitation wavelength. The pupil function, after including defocus and aberrations, can be written as

$$P(k_x,k_y,z) = \begin{cases} \exp(jk_0\varphi(\theta_i,\theta_s,z)), & \text{if } \frac{(k_x^2+k_y^2)^{\frac{1}{2}}}{k_i} < \frac{NA}{n_i}\,, \\ 0, & \text{otherwise}\,, \end{cases} \tag{2}$$

where $\mathrm{NA} = n_i \sin\alpha$, and α is the maximum semi-aperture angle so that $\theta_i \leq \alpha$. $\varphi(\theta_i,\theta_s,z)$ is the optical phase difference between the wavefront emerging from the exit pupil and a reference wave. In the above expression, the amplitude of the pupil function is approximated to be a constant. θ_s is the angle in the object plane related to θ_i by Snell's law as $n_i \sin\theta_i = n_s \sin\theta_s$, and n_s is the refractive index of the specimen medium.

The phase $\varphi(\theta_i,\theta_s,z)$ is the sum of the defocus term $\varphi_d(\theta_i,z)$ and the aberration phase $\varphi_a(\theta_i,\theta_s)$. P. A. Stokseth [9] gave the expression for this defect of focus as:

$$\varphi_d(\theta_i,z;n_i) \approx n_i z(1-\cos\theta_i)\,. \tag{3}$$

In this case, as the medium between the lens and the specimen is air, $n_i = 1.0$. For a widefield MACROscope, the emission amplitude PSF, $h_{\mathrm{A}}(\mathbf{x};\lambda_{\mathrm{em}})$, could be assumed to be close to the excitation amplitude PSF, $h_{\mathrm{A}}(\mathbf{x};\lambda_{\mathrm{ex}})$, so that they are related to the magnitude PSF, $h(\mathbf{x})$, by

$$h(\mathbf{x}) = |h_{\mathrm{A}}(\mathbf{x};\lambda_{\mathrm{ex}})|^2. \tag{4}$$

In the entire expression for $h(\mathbf{x})$, as the only unknown is the phase $\varphi_a(\theta_i,\theta_s)$ from the aberrations, the problem of phase retrieval is a question of estimating the aberrated phase from the observed intensities. As we are working on a MACROscope under low NA, the effect of polarization can be neglected and a scalar diffraction model is sufficient.

2.1. Maximum likelihood algorithm

If we consider the assumption of Poissonian photon counting statistics [see 10], the observation can be written as:

$$i(\mathbf{x}) = \mathcal{P}\{|h_{\mathrm{A}}(\mathbf{x})|^2 + b(\mathbf{x})\}\,, \forall \mathbf{x} \in \Omega_s\,, \tag{5}$$

where $b(\mathbf{x})$ is the low-frequency background signal [10]. In the above expression, we assume that the fluorescent bead can be considered as a point source. The background, $b(\mathbf{x})$, can be estimated either from a single dark image of the CCD or from the histogram.

To estimate the amplitude PSF, $h_{\mathrm{A}}(\mathbf{x})$, from the intensity image, $i(\mathbf{x})$, we use Bayesian inferencing. From the Bayes' theorem, the posterior probability is

$$\Pr(h_{\mathrm{A}}|i) = \frac{\Pr(i|h_{\mathrm{A}})\Pr(h_{\mathrm{A}})}{\Pr(i)}\,, \tag{6}$$

where $\Pr(h_{\mathrm{A}})$ is a p.d.f, the prior from which h_{A} is assumed to be generated. $\Pr(i|h_{\mathrm{A}})$ is the likelihood function for the PSF and it specifies the probability of obtaining an image $i(\mathbf{x})$ from a diffraction-limited point source:

$$\Pr(i|h_{\mathrm{A}}) = \prod_{\mathbf{x}\in\Omega_s} \frac{(h_{\mathrm{A}}+b)(\mathbf{x})^{i(\mathbf{x})}\exp(-(h_{\mathrm{A}}+b)(\mathbf{x}))}{i(\mathbf{x})!}\,. \tag{7}$$

An estimate of the near-focus amplitude distribution, $\hat{h}_{\mathrm{A}}$, can be obtained by using the maximum a posteriori (MAP) estimate or by minimizing the cologarithm of the *a posteriori* as

$$\begin{aligned} \hat{h}_{\mathrm{A}}(\mathbf{x}) &= \underset{h_{\mathrm{A}}(\mathbf{x})}{\operatorname{argmax}} \Pr(h_{\mathrm{A}}|i),\ \text{s. t. } k_{\mathrm{MAX}} < \frac{2\pi\mathrm{NA}}{\lambda_{\mathrm{ex}}}\,, \\ &= \underset{h_{\mathrm{A}}(\mathbf{x})}{\operatorname{argmin}} -\log[\Pr(h_{\mathrm{A}}|i)],\ \text{s. t. } k_{\mathrm{MAX}} < \frac{2\pi\mathrm{NA}}{\lambda_{\mathrm{ex}}}\,, \end{aligned} \tag{8}$$

where k_{MAX} is the maximum frequency permissible by the pupil of the imaging system. As $\Pr(i(\mathbf{x}))$ does not depend on $h_{\mathrm{A}}(\mathbf{x})$, it can be considered as a normalization constant, and it shall hereafter be excluded from all the estimation procedures. The minimization of the cologarithm of $\Pr(h_{\mathrm{A}}|i)$ in Eq. (6) can be rewritten as the minimization of the following joint energy functional:

$$\mathcal{J}(h_{\mathrm{A}}|i) = -\log[\Pr(h_{\mathrm{A}}|i)] = \underbrace{\mathcal{J}_{\mathrm{obs}}(i|h_{\mathrm{A}})}_{\text{Image energy}} + \underbrace{\mathcal{J}_{\mathrm{reg},h_{\mathrm{A}}}(h_{\mathrm{A}})}_{\text{Prior energy}}\,. \tag{9}$$

$\mathcal{J}_{\mathrm{obs}}\colon \Omega_s \mapsto \mathbb{C}$ is a measure of fidelity to the data and it corresponds to the cologarithm of the term $\Pr(i|h_{\mathrm{A}})$ from the noise distribution. It has the role of pulling the solution towards the observation data. We make a decision about the underlying scene based on this cost function, and it specifies the penalty paid by the system in producing an incorrect estimate of the scene. $J_{\mathrm{reg},h_{\mathrm{A}}} : \Omega_s \mapsto \mathbb{R}$ corresponds to the penalty term $\Pr(h_{\mathrm{A}})$ that ensures smoothness of the solution. For the GS algorithm, as there is no intrinsic smoothness term, to compare our approach with the GS algorithm, we drop the prior energy term in Eq. (6) (by assuming a uniform distribution). The amplitude PSF can be estimated by the maximum likelihood (ML) algorithm:

$$\begin{aligned} \hat{h}_{\mathrm{A}}(\mathbf{x}) &= \underset{h_{\mathrm{A}}(\mathbf{x})}{\operatorname{argmin}}\, \mathcal{J}_{\mathrm{obs}}(i|h_{\mathrm{A}})\,,\ \text{s. t. } k_{\mathrm{MAX}} < \frac{2\pi\mathrm{NA}}{\lambda_{\mathrm{ex}}} \\ &= \underset{h_{\mathrm{A}}(\mathbf{x})}{\operatorname{argmin}} -\log[\Pr(i|h_{\mathrm{A}})],\ \text{s. t. } k_{\mathrm{MAX}} < \frac{2\pi\mathrm{NA}}{\lambda_{\mathrm{ex}}}\,, \\ &= \underset{h_{\mathrm{A}}(\mathbf{x})}{\operatorname{argmax}} |h_{\mathrm{A}}(\mathbf{x})|^2 - i(\mathbf{x})\log\left(|h_{\mathrm{A}}(\mathbf{x})|^2 + b(\mathbf{x})\right), \\ &\text{s. t. } k_{\mathrm{MAX}} < \frac{2\pi\mathrm{NA}}{\lambda_{\mathrm{ex}}}\,. \end{aligned} \tag{10}$$

As there is no closed-form solution to the above problem, we use the following fixed-point iterative algorithm:

$$\hat{h}_{\mathrm{A}}^{(n+1)}(\mathbf{x}) = \hat{h}_{\mathrm{A}}^{(n)} - \tau\frac{\partial}{\partial h_{\mathrm{A}}(\mathbf{x})}\mathcal{J}_{\mathrm{obs}}(i|h_{\mathrm{A}})\,. \tag{11}$$

In the above iterative step, $\tau \in [0,1]$ is a scaling factor and the gradient of the cost function in Eq. (11) is

$$\begin{aligned}\frac{\partial}{\partial h_{\mathrm{A}}}\mathcal{J}_{\mathrm{obs}}(i|h_{\mathrm{A}}) &= \frac{\partial}{\partial h_{\mathrm{A}}}\{|h_{\mathrm{A}}|^2 + b - i\log|\Big(h_{\mathrm{A}}|^2 + b\Big)\}\,, \\ &= \left(h_{\mathrm{A}}(-\mathbf{x}) - \frac{i(\mathbf{x})}{(|h_{\mathrm{A}}(\mathbf{x})|^2 + b(\mathbf{x}))}h_{\mathrm{A}}(-\mathbf{x})\right), \\ &\forall \mathbf{x} \in \Omega_s\,. \end{aligned} \tag{12}$$

where $h_{\mathrm{A}}(-\mathbf{x})$ is the complex conjugate transpose of $h_{\mathrm{A}}(\mathbf{x})$. From Eq. (11) and (12) we get the fixed-point iterative algorithm for the near-focus amplitude PSF as

$$\hat{h}_{\mathrm{A}}^{(n+1)}(\mathbf{x}) = \hat{h}_{\mathrm{A}}^{(n)}(\mathbf{x}) - \tau\times \left(\hat{h}_{\mathrm{A}}^{(n)}(-\mathbf{x}) - \frac{i(\mathbf{x})}{\left(|\hat{h}_{\mathrm{A}}^{(n)}(\mathbf{x})|^2 + b(\mathbf{x})\right)}\hat{h}_{\mathrm{A}}^{(n)}(-\mathbf{x})\right)\,, \tag{13}$$

$\forall \mathbf{x} \in \Omega_s$. For the above iterations, the initial pupil function, $\hat{P}^{(0)}(k_x,k_y,z=0)$, is chosen to be a disc with a maximum radius of k_{MAX} and phase zero (*cf.* Eq. (2)). This is inverse Fourier transformed to get $\hat{h}_{\mathrm{A}}^{(0)}(\mathbf{x})$ (*cf.* Eq. (1)). The iterations are done until either the mean-squared error (MSE) between the phase estimates for two successive iteration is below a certain value or a certain number of iterations is reached by the algorithm. It is important to note that although the given observation is real, the final estimate $\hat{h}_{\mathrm{A}}(\mathbf{x})$ is complex.

2.2. The Gerchberg-Saxton algorithm

The GS algorithm is a pupil phase estimation technique of forward and inverse Fourier transforms on the observation. This problem of phase retrieval is normally under-determined. However, as the phase that is to be estimated does not change with defocus, it can be estimated if images of point source at multiple defocus positions are available. The only requirement is that these sections are as far away as possible from the central defocus section. This is because, the extremity sections have more information about the conjugate plane than the center. As the distance from the center tends towards infinity, the intensity slice at infinity directly gives the back pupil plane. However, the measurement of defocused beads becomes increasingly difficult in practice for larger defocusing due to the decaying intensity with z, which imposes a compromise.

The initialization of the pupil function is same as that for the fixed-point iterative algorithm. A suitable phase curvature is added to this complex pupil function to obtain the defocus adjusted complex pupil function, $P(k_x,k_y,z)$, at every defocus z. This is inverse Fourier transformed (*cf.* Eq. (4)) to get the corresponding amplitude PSF ($h_{\mathrm{A}}(\mathbf{x})$) intensities at the different defocus planes. The magnitude of $h_{\mathrm{A}}(x)$ is assigned to the corresponding measured intensities (after background subtraction) at the different defocus planes. A Fourier transform of this modified $h_{\mathrm{A}}(x)$ gives the new estimate of the defocus-adjusted complex exit pupil function, $\hat{P}(k_x,k_y,z)$, at the different defocus positions of z. The resulting defocus-adjusted complex pupil functions are readjusted back to zero and averaged to get a new estimate of the complex exit pupil function $\hat{P}(k_x,k_y,z=0)$. This process is repeated until the MSE criterion or the maximum iteration is reached. Some constraints are introduced during the iterative algorithm that can aid in the convergence of the algorithm. The progress of the fixed-point algorithm is same as the GS algorithm except for Step 5 in Algorithm 1. We see that when $\tau = 1$ in Eq. (12), then the factor $i(x)/(|\hat{h}_{\mathrm{A}}^{(n)}(\mathbf{x})|^2 + b(\mathbf{x}))$, at each iteration, performs the assigning operation of Step 5.

begin
- **Input**: Observed: M defocus sections i$(\mathbf{x})$, $\forall \mathbf{x} \in \Omega_s$.
- **Data**: Maximum iteration n_{MAX}.
- **Output**: Complex pupil function $\hat{P}(k_x,k_y,z=0)$.
- 1. Initialization: $n \leftarrow 0$, calculate $\hat{P}^{(n)}(k_x,k_y,z=0)$ (*cf.* Eq. (2)).
- 2. Preprocessing: Estimate background $\hat{b}$.
- $i(\mathbf{x}) \leftarrow i(\mathbf{x}) - \hat{b}$ and set $i(\mathbf{x}) = \{0 : \text{forall } i(\mathbf{x}) < 0\}$.
- **while** $n \leq n_{MAX}$ **do**
  - **while** $m \leq M$ **do**
    - 3. Adjust defocus: $\hat{P}^{(n)}(k_x,k_y,z(m)) \leftarrow \hat{P}^{(n)}(k_x,k_y,z(m))\exp(i\varphi_d(k_x,k_y,z(m)))$ (*cf.* Eq. (3)).
    - 4. Pupil to PSF: $\hat{h}_{\mathrm{A}}^{(n)}(\mathbf{x}) \leftarrow \mathcal{F}_{\mathrm{2D}}^{-1}\{\hat{P}^{(n)}(k_x,k_y,z)\}$
    - 5. Assign: $|\hat{h}_{\mathrm{A}}^{(n)}(\mathbf{x})| \leftarrow (i(\mathbf{x}))^{1/2}$.
    - 6. PSF to pupil: $\hat{P}^{(n+1)}(k_x,k_y,z) \leftarrow \mathcal{F}_{\mathrm{2D}}\{\hat{h}_{\mathrm{A}}^{(n)}(\mathbf{x})\}$.
    - 7. Readjust defocus: $\hat{P}^{(n+1)}(k_x,k_y,z) \leftarrow \hat{P}^{(n+1)}(k_x,k_y,z)\exp(-i\varphi_d(k_x,k_y,z))$.
    - 8. Projection: Impose NA limit on $\hat{P}^{(n+1)}(k_x,k_y,z)$ to remove higher frequencies.
  - **end**
- **end**

end

Algorithm 1: The Gerchberg-Saxton algorithm.

3. RESULTS AND DISCUSSION

For the experiments, we chose fluorescent microspheres of size 2.5μm from Molecular Probes'. We diluted a 1μl of this suspension in 20μl of distilled water and dried a drop of this on to a coverslip. These dried beads were then imaged using a Leica$^{\mathrm{TM}}$ MacroFluo$^{\mathrm{TM}}$ fit with a 5$\times$ planapochromatic HR objective and 16 zoom positions. The maximum NA of this system is 0.5. Two zoom positions are considered at 9.2$\times$ (radial sampling 178.33nm and axial sampling 1000nm), and 1.6$\times$ (radial sampling 998.3nm and axial sampling 1000nm).

Given the fact that the MACROscope works under a variable zoom, the NA of the optical mount is variable. If we consider the light as a cone, the apex of the cone is at the central observed intensity plane and the base of the cone is the observed diffraction ring at a defocus plane of distance H away from the center. D is the diameter of the largest concentric ring of the base. For the observed intensities in Fig. 2(a)/(b), for a zoom of 9.2$\times$, the maximum radius of the diffractive ring pattern at a distance of $H = 61\mu$m away from the center was measured to be about 32.46μm. The measured radius $D/2$ is related to the angle α and the defocus distance H by $tan(\alpha) = D/2H = 32.46/61 = 0.53$. The maximum subtended semi-cone angle will be $\alpha = \arctan(0.53) = 0.49$ radians. Since $n_i = 1$, the effective NA can be calculated to be about 0.47 which is closer to the manufacture specified NA of 0.5. If we consider another set of images taken under a zoom of 1.6$\times$, D was measured to be 32.70μm for a H of 71μm. In this case the NA was calculated as

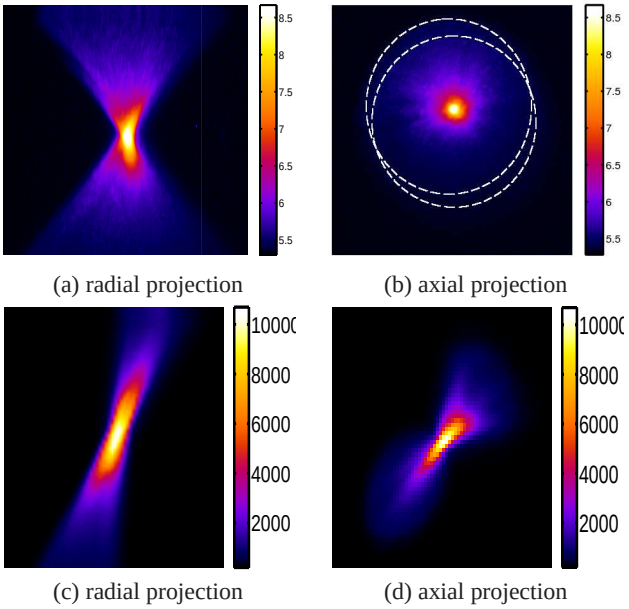

(a) radial projection (b) axial projection

(c) radial projection (d) axial projection

Fig. 2. Radial and axial intensity projection of a 2.5μm fluorescent bead on a log scale. The beads were imaged using a Leica^{TM} MacroFluo^{TM}. (a) and (b) are taken from the field centre, and at a zoom 9.2$\times$ with a radial sampling of 178.33nm and axial sampling of 1000nm. The projection along the radial plane shows the overlap region marked in white. (c) and (d) are taken from the periphery, and at a zoom 1.6$\times$ with a radial sampling of 998.3nm and axial sampling of 1000nm.

0.22. We use these two calculated NA values to limit the frequency bandwidth in the pupil plane of Eq. (1).

Four defocus sections were chosen above and below the central defocus reference plane of the 1.6$\times$ image that is shown in Fig. 2(c)/(d). This bead is cropped from the periphery of the field. One of the defocus sections is shown in Fig. 3(a). The wrapped phase

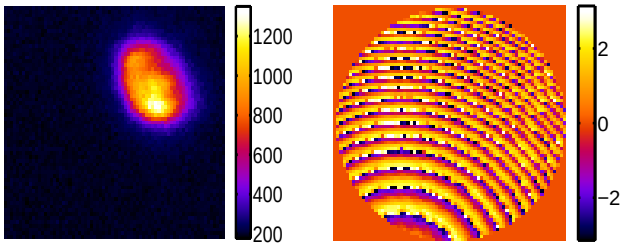

(a) (b)

Fig. 3. (a) The first section of the observed intensity, $z = -57\mu$m, and (b) retrieved wrapped pupil phase from the intensity images of Fig. 2(c), (d). $\tau = 0.6$ and the maximum number of iteration is 1000.

of the pupil is retrieved after about 1000 iterations of the fixed-point algorithm, with $\tau = 0.6$, is shown in Fig. 3(b). In order to reduce noisy estimates, at each iteration, the estimate obtained from the GS algorithm is filtered by a Gaussian filter with a standard-deviation $\sigma = 356.66$nm. However, this is an *ad hoc* method. Instead, at each iteration of the fixed-point iterative algorithm, the estimated pupil function is regularized by a total variation functional [see 10]. We noticed that the solution relatively stabilizes after about 300 iterations and does not deteriorate any further.

From the estimated phase, we see that the pupil function of the optical system is chopped. This chopping of the pupil, or the 'cat's' eye effect [see 11], is a result of two limiting apertures (the objective and the zoom) brought together without any tele-centric correction. This effect can also be seen in the axial projection in Fig. 2(b), and in the defocus section of Fig. 3(a). For ease of understanding, the defocus projection of the image is demarcated with two white circles to show that the PSF axis is not parallel to the optical axis. Our future work is aimed at correcting this field aberration computationally.

4. REFERENCES

[1] P. Sendrowski and C. Kress, "Arrangement for analyzing microscopic and macroscopic preparations," WO 2009/04711, Apr. 2009, PCT/EP2008/062749. 1

[2] L. Sherman, J. Y. Ye, O. Albert, and T. B. Norris, "Adaptive correction of depth-induced aberrations in multiphoton scanning microscopy using a deformable mirror," *J. Microsc.*, vol. 206, no. 1, pp. 65–71, 2002. 1

[3] M. J. Booth, M. A. Neil, R. Juškaitis, and T.Wilson, "Adaptive aberration correction in a confocal microscope," *Proc. Natl. Acad. Sci.*, vol. 99, no. 9, pp. 5788–5792, 2002. 1

[4] Z. Kam, P. Kner, D. Agard, and J. W. Sedat, "Modelling the application of adaptive optics to wide-field microscope live imaging," *J. Microsc.*, vol. 226, pp. 33–42, 2007. 1

[5] M. J. Booth, "Adaptive optics in microscopy," *Philos. Transact. A Math. Phys. Eng. Sci.*, vol. 365, no. 1861, pp. 2829–2843, Dec. 2007. 1

[6] R. Juškaitis and T. Wilson, "The measurement of the amplitude point spread function of microscope objective lenses," *J. Microsc.*, vol. 189, no. 1, pp. 8–11, 1998. 1

[7] R. W. Gerchberg and W. O. Saxton, "A practical algorithm for the determination of the phase from image and diffraction plane pictures," *Optik*, vol. 35, pp. 237–246, 1972. 1

[8] M. Born and E. Wolf, *Principles of Optics*, Cambridge U. Press, 1999. 2

[9] P. A. Stokseth, "Properties of a defocused optical system," *J. Opt. Soc. Am. A*, vol. 59, pp. 1314–1321, Oct. 1969. 2

[10] P. Pankajakshan, *Blind Deconvolution for Confocal Laser Scanning Microscopy*, Ph.D. thesis, Université de Nice Sophia-Antipolis, Dec. 2009. 2, 4

[11] P. Pankajakshan, Z. Kam, A. Dieterlen, G. Engler, L. Blanc-Féraud, J. Zerubia, and J.-C. Olivo-Marin, "Point-spread function model for fluorescence macroscopy imaging," in *Proc. of Asilomar Conference on Signals, Systems and Computers*, Nov. 2010, to be published. 4